WG1 - S11 [^{1}H(p,$e^+\nu$)^{2}H] and theory, extrapolations, radiative corrections, electron capture, neutrino spectra

Jiunn-Wei Chen (Natl. Univ. Taiwan)
Laura E. Marcucci (Univ. Pisa - INFN Pisa)

Summary

- Introduction: some definitions
- Fitting and extrapolating S-factors
- The *pp* (and *hep*) reaction $\rightarrow$
  - radiative corrections
  - theoretical approaches
- Electron capture by ^{7}Be & *pep*
- Neutrino spectra $\longrightarrow$ WG2, THANKS!

For each item $\rightarrow$

1. review SFII
   Adelberger *et al.*, RMP **83**, 195 (2011)
2. review work done after SFII

Many thanks to the WG1 participants for their help!
My apologize if I still forgot someone/something!

Introduction: some definitions (I)

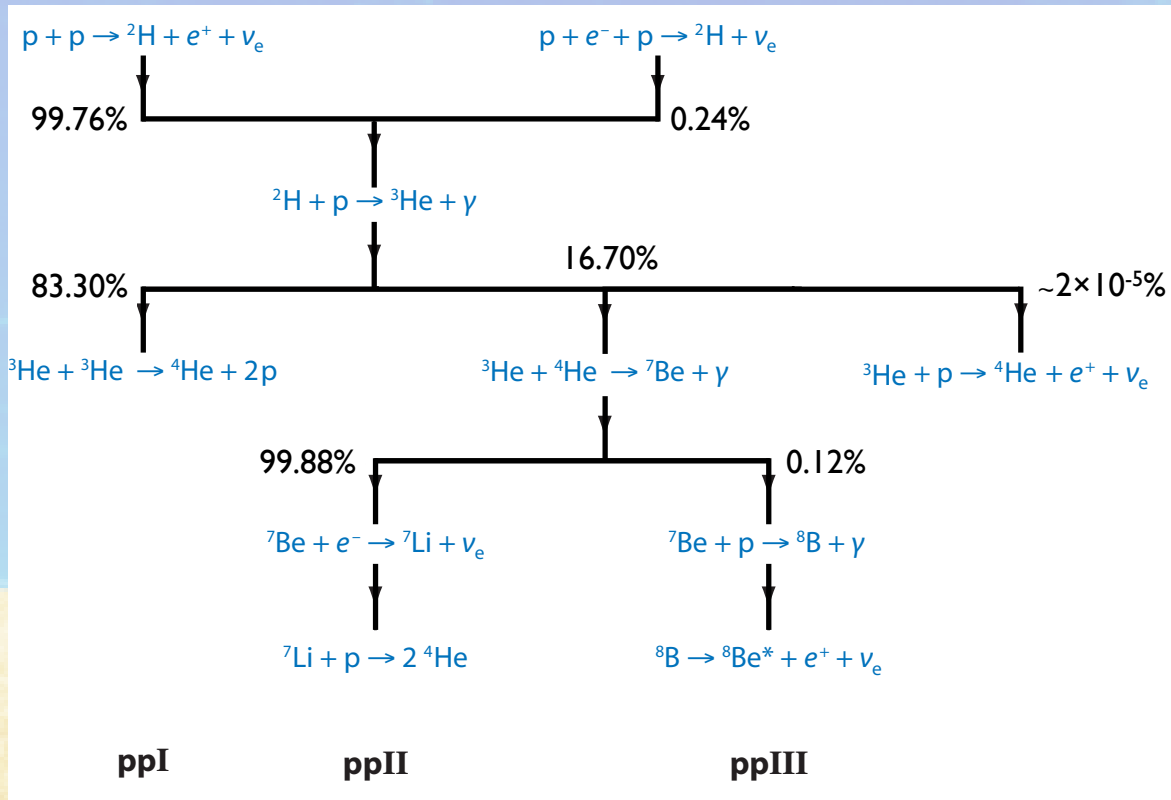

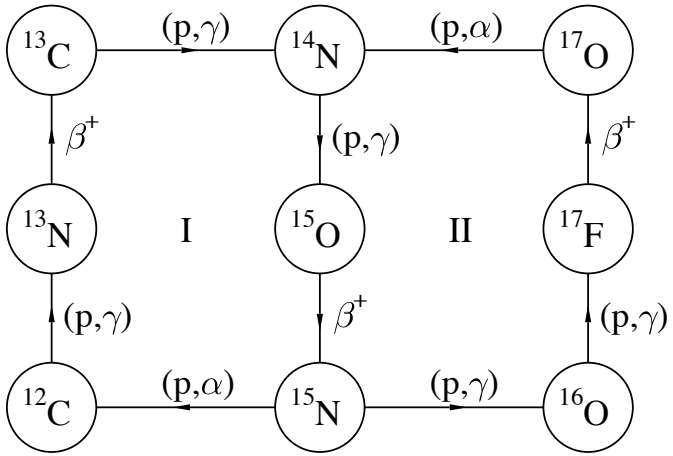

$$r_{12} = \frac{n_1\, n_2}{1+\delta_{12}}\,\langle\sigma v\rangle_{12}$$

$$\langle\sigma v\rangle_{12} = \int_0^\infty \sigma(v)\; v\; \Phi(v)\,\mathrm{d}v \qquad \Phi(v) = \mathrm{Maxwell-Boltzmann\ distrib.}$$

$$\langle\sigma v\rangle_{12} = \sqrt{\frac{8}{\pi\mu(kT)^3}}\int_0^\infty E\;\sigma(E)\;\exp\left(-\frac{E}{kT}\right)\;\mathrm{d}E$$

Introduction: some definitions (II)

$$\sigma(E) = \frac{S(E)}{E} \exp[-2\pi\eta(E)] \qquad \eta(E) = Z_1 Z_2 \alpha / v$$

$S(E)$ known $\rightarrow$

$$\langle \sigma v \rangle_{12} = \sqrt{\frac{8}{\pi \mu (kT)^3}} \int_0^\infty S(E) \exp\left[-\frac{E}{kT} - 2\pi\eta(E)\right]$$

Taylor exp. $\rightarrow$

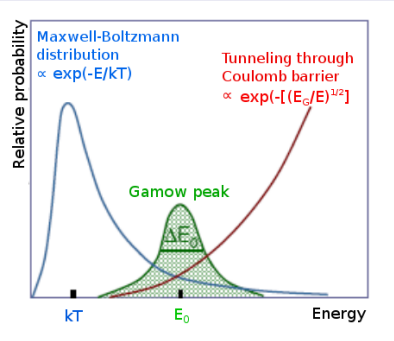

$$\langle \sigma v \rangle_{12} = \sqrt{\frac{2}{\mu kT}} \frac{\Delta E_0}{kT} f_0 \, S_{\rm eff} \exp[-3E_0/(kT)]$$

$$E_0 = \text{Gamow peak}$$

$$\frac{\Delta E_0}{kT} = 4\sqrt{\frac{E_0}{3kT}}$$

$$f_0 = \text{electron screening}$$

$$S_{eff} = S(0)\left(1 + \frac{5kT}{36E_0}\right) + S'(0)E_0\left(1 + \frac{35kT}{36E_0}\right) + \frac{1}{2}S''(0)E_0^2\left(1 + \frac{89kT}{36E_0}\right)$$

Fitting and extrapolating S-factors (I)

SFII

- $S(0), S'(0), S''(0) \rightarrow$ **quadratic fit to data**, typically valid up to few hundreds keV $\Rightarrow$ no theoretical justification
- Theory constraints:
  1. peripheral nature of non-resonant capture
  2. model-based calculations (cluster approach)
  3. R-matrix approach
  4. *ab-initio* calculations
- Adopted procedure:
  - *pp* & *hep* $\rightarrow$ theory [no data]
  - if data $\exists$ and adequate $\rightarrow$ polynomial fit of the data
  - if data $\exists$ but not adequate $\rightarrow$ fitting function [theory] + normalization [data]

Fitting and extrapolating S-factors (II)

After SFII

- Gaspard, Sparenberg, Wenda, Baye, PRC **100**, 035805 (2019) $\rightarrow$ *pp* capture $\rightarrow$ see below
- **Halo-EFT + Bayesian methods** (Markov Chain Monte Carlo sampling)
  - $^{7}\mathrm{Li}(n,\gamma)^{8}\mathrm{Li}$
    - Zhang, Nollett, Phillips, PRC **89**, 024613 (2014)
    - Rupak & Higa, PRL **106**, 222501 (2011)
  - $^{7}\mathrm{Be}(p,\gamma)^{8}\mathrm{B}$
    - Zhang, Nollett, Phillips, PRC **89**, 051602(R) (2014); PLB **751**, 535 (2015); PRC **98**, 034616 (2018)
    - Higa, Premarathna, Rupak, PRC **106**, 014601 (2022)
  - $^{3}\mathrm{He}(^{4}\mathrm{He},\gamma)^{7}\mathrm{Be}$
    - Zhang, Nollett, Phillips, JPG **47**, 054002 (2020)
    - Higa, Rupak, Vagnani, EJPA **54**, 89 (2018); Premarathna & Rupak, EPJA **56**, 166 (2020)
- ***R*-matrix+Bayesian methods** (BRICK - Bayesian *R*-matrix Inference Code Kit)
  - $^{3}\mathrm{He}(^{4}\mathrm{He},\gamma)^{7}\mathrm{Be}$; $^{3}\mathrm{He}(\alpha,\alpha)^{3}\mathrm{He}$
    - Odell *et al.*, FP **10**, 888476 (2022)

Halo-EFT + Bayesian methods

- $S(E) = f(\mathrm{LECs})$ from halo-EFT
- LECs fitted to exp. data via Bayesian methods
- predict $S(E)$ $\forall$ E

Zhang, Nollett, Phillips, PLB **751**, 535 (2015)

Table 2
The median values of S, S'/S, and S''/S at $E = 0$ keV [$E = 20$ keV], as well as the upper and lower limits of the (asymmetric) 68% interval. The sampling errors are 0.02%, 0.07%, 0.01% for median values, as estimated from $\langle X^2 - \langle X \rangle^2 \rangle^{1/2} / \sqrt{N}$ with $N = 2 \times 10^4$.

	S (eV b)	S'/S (MeV^{-1})	S''/S (MeV^{-2})
Median	21.33 [20.67]	−1.82 [−1.34]	31.96 [22.30]
$+\sigma$	0.66 [0.60]	0.12 [0.12]	0.33 [0.34]
$-\sigma$	0.69 [0.63]	0.12 [0.12]	0.37 [0.38]

$$p + {}^7\mathrm{Be} \to {}^8\mathrm{B} + \gamma$$

$$[S_{17}(0)]_{\mathrm{SFII}} \quad 20.8 \pm 1.6 \text{ eV b}$$
$$[S'_{17}(0)/S_{17}(0)]_{\mathrm{SFII}} \quad -1.5 \pm 0.1 \text{ MeV}^{-1}$$
$$[S''_{17}(0)/S_{17}(0)]_{\mathrm{SFII}} \quad 11 \pm 4 \text{ MeV}^{-2}$$

Higa, Premarathna, Rupak, PRC **106**, 014601 (2022)

TABLE III. S_{17} and its first two energy derivatives at $E_0 = 50 \times 10^{-3}$ keV. The first set of errors are from the fits. The second set is the estimated LO 30%, NLO 10%, and NNLO 3% EFT errors, respectively, from higher-order corrections.

Theory	S_{17} (eV b)	S'_{17}/S_{17} (MeV^{-1})	S''_{17}/S_{17} (MeV^{-2})
EFT$_{\mathrm{gs}}$/EFT$_\star$ I LO	24.4(3)(73)	−2.44(5)(73)	35.8(7)(108)
EFT$_{\mathrm{gs}}$/EFT$_\star$ I NLO	21.1(3)(21)	−1.87(4)(19)	32.4(6)(32)
EFT$_{\mathrm{gs}}$ I NNLO	20.7(3)(6)	−1.79(4)(5)	31.9(6)(10)
EFT$_\star$ I NNLO	20.9(4)(6)	−1.82(8)(5)	31.9(8)(10)
EFT$_\star$ II LO	24.8(3)(74)	−2.44(4)(73)	35.8(6)(108)
EFT$_\star$ II NLO	19.8(2)(20)	−1.91(3)(19)	32.7(5)(33)
EFT$_\star$ II NNLO	21.2(3)(6)	−1.89(4)(6)	31.9(6)(10)

$S_{17}(0) = 21.0(7)$ eV b S''_{17}/S_{17} larger than SFII by a factor of 3

R-matrix + Bayesian methods (BRICK)

- Pheno R-matrix challenge: estimate of uncertainties on cross sections and fit parameters
- Use Markov Chain Monte Carlo sampler + R-matrix → BRICK
- Applied to $^3\mathrm{He}(\alpha,\gamma)^7\mathrm{Be}$ and $^3\mathrm{He}(\alpha,\alpha)^3\mathrm{He}$

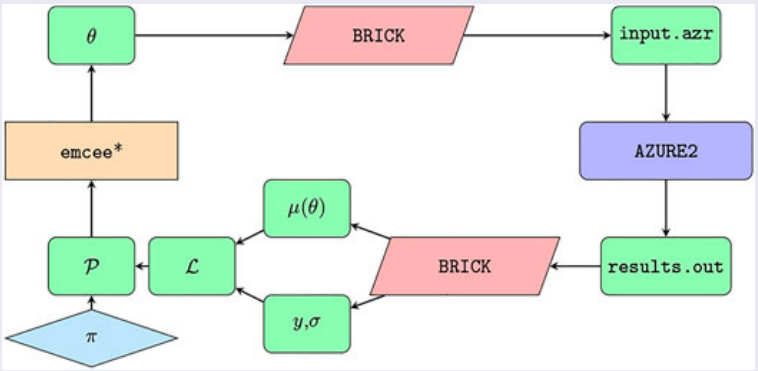

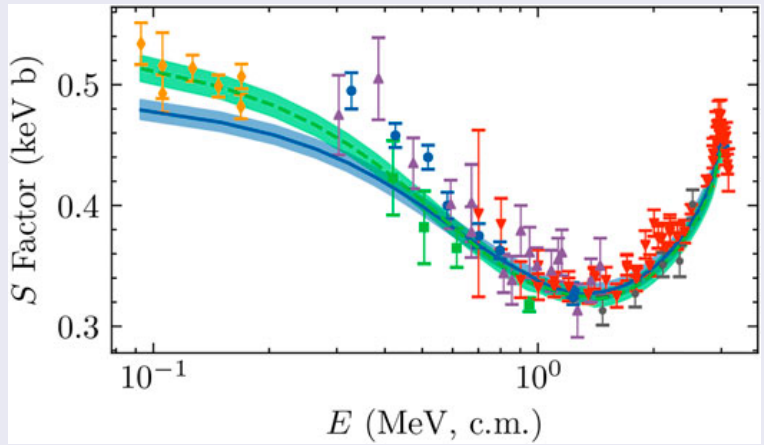

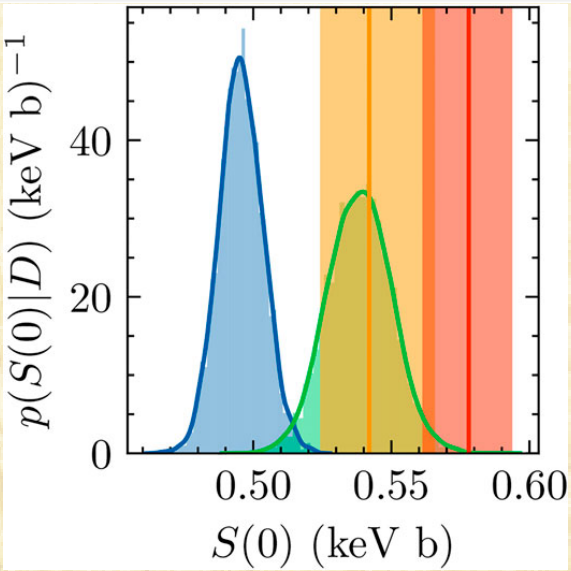

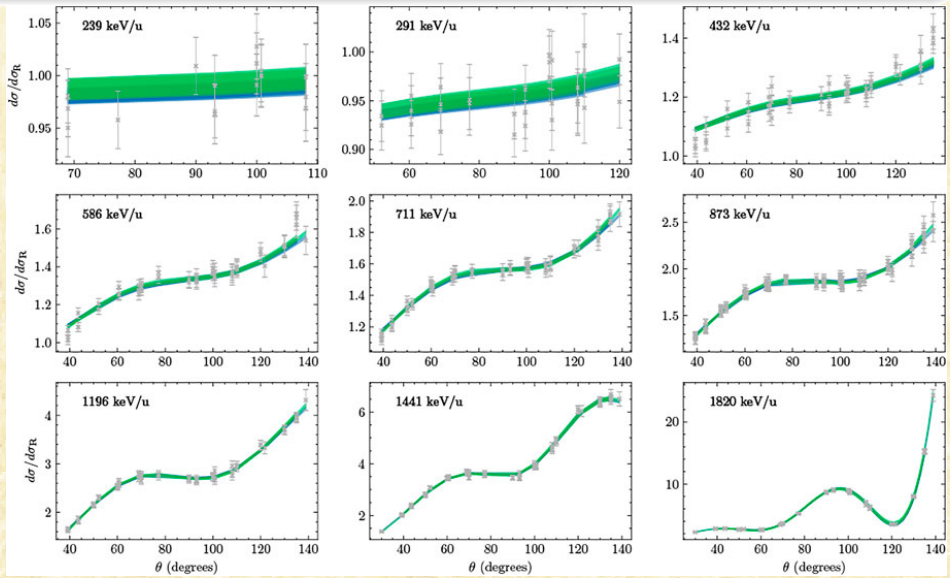

Odell *et al.*, FP **10**, 888476 (2022)

In conclusion:

If in SFIII we want ...

1. ... a general statement
   $\Rightarrow$ Need help from ALL participants!
   $\Rightarrow$ Maybe need to reserve some time in plenary session

2. ... different prescription for each reaction
   $\Rightarrow$ WG1 will take care of *pp* reaction

The *pp* reaction: SFII (I)

$$S_{11}(0) = 4.01 \times 10^{-25}\,\mathrm{MeV\ b} \left(\frac{(ft)_{0^+\to 0^+}}{3071\,\mathrm{s}}\right)^{-1} \left(\frac{G_A/G_V}{1.2695}\right)^{2} \left(\frac{f_{pp}^R}{0.144}\right) \left(\frac{\overline{\Lambda}^2}{7.035}\right)$$

- $(ft)_{0^+\to 0^+} = 3071.4 \pm 0.8$ s from Hardy & Towner PRC **79**, 055502 (2009)
- $G_A/G_V = 1.2695 \pm 0.0029$ from PDG
- $f_{pp}^R = 0.144(1 \pm 0.001)$ phase-space factor **with radiative corrections**
- $\overline{\Lambda}^2$ = transition matrix element between initial *pp* and final *d* states
  - $\overline{\Lambda}^2 = 7.035(1 \pm 0.009) \rightarrow$ potential models
  - $\overline{\Lambda}^2 = 7.03(1 \pm 0.008) \rightarrow$ EFT*
  - $\overline{\Lambda}^2 = 6.99 \pm 0.21 \rightarrow \not$EFT

$$S_{11}(0) = \begin{array}{lll} 4.01(1 \pm 0.009) \times 10^{-25} & \mathrm{MeV\ b} & \text{potential models} \\ 4.01(1 \pm 0.009) \times 10^{-25} & \mathrm{MeV\ b} & \mathrm{EFT}^* \\ 3.99(1 \pm 0.030) \times 10^{-25} & \mathrm{MeV\ b} & \not\mathrm{EFT} \end{array}$$

Recommended value: $S_{11}(0) = 4.01(1 \pm 0.009) \times 10^{-25}\,\mathrm{MeV\ b}$

For $S'_{11}(0) \rightarrow S'_{11}(0) = S_{11}(0)(11.2 \pm 0.1)\,\mathrm{MeV}^{-1}$ from Bahcall & May, ApJ **155**, 501 (1969)

The *pp* reaction: SFII (II)

Theoretical approaches

- Potential models: $V_{NN} + j^A(\boldsymbol{q}) \rightarrow$ phenom. accurate models (MECs fitted to ^{3}H β-decay)
- EFT*: $V_{NN} \rightarrow$ phenom. models $+ j^A(\boldsymbol{q}) \rightarrow \chi$EFT (LEC d_R fitted to ^{3}H β-decay)
- $\not\pi$EFT: EFT with π's integrated out + systematic expansion in (q/m_π) up to N4LO; $j^A(\boldsymbol{q}) \rightarrow L_{1,A}$ at N2LO from several NN systems (SNO+SK solar ν flux data)

Radiative corrections (RCs)

- $f_{pp} = 0.142 \rightarrow$ Bahcall & May, ApJ **155**, 501 (1969)
- increase of 1.62% due to RCs [Fig. (a)]
  $\rightarrow$ Kurylov, Ramsey-Musolf, Vogel, PRC **67**, 035502 (2003)
- estimated error of $\sim 0.1\%$ [Fig. (b)]

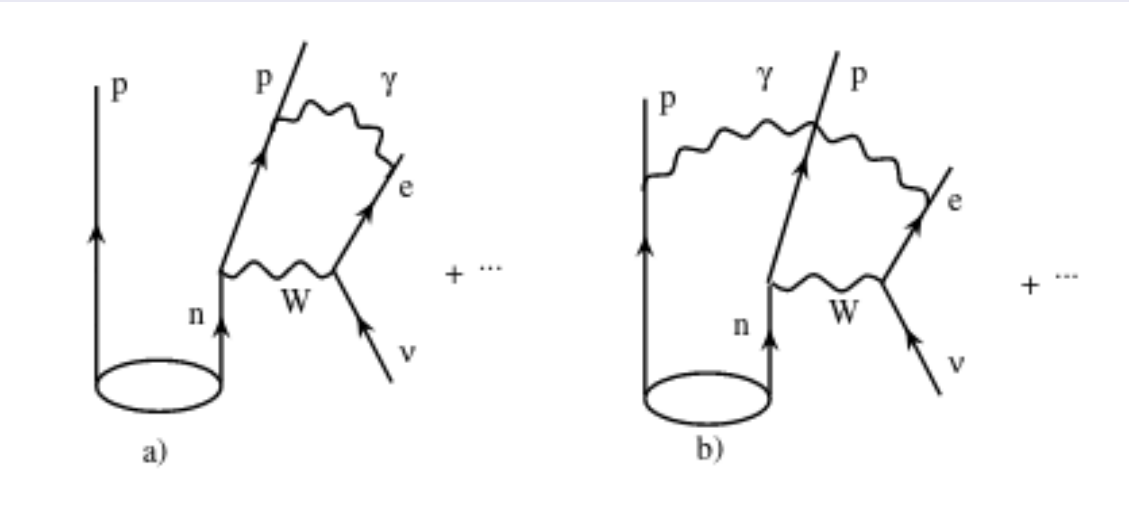

The *pp* reaction: SFII (III)

Recommendations

- calculate (b)-diagrams and confirm f_{pp}^{R}
- Full χEFT calculations
- $L_{1,A}$ in $\not\pi$EFT $\rightarrow$ muon capture on deuteron (MuSun exp.)

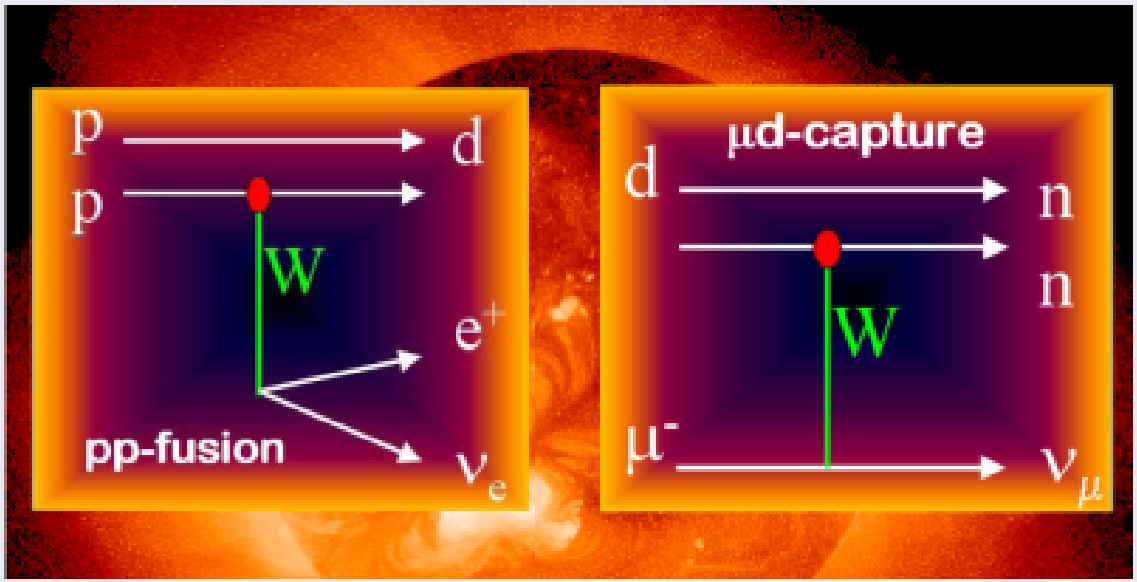

- Modern calculation for $S'_{11}(0)$ & $S''_{11}(0)$

After SFII: RCs

- **no (b)-diagrams calculation yet** (work in progress)
- Czarnecki, Marciano, Sirlin, PRL **120**, 202002 (2018); PRD **100**, 073008 (2019)

$\tau_n^{\rm beam} = 888.0(2.0)$ s vs. $\tau_n^{\rm trap} = 879.4(6)$

$g_A^{\rm pre2002} = 1.2637(21)$ vs. $g_A^{\rm post2002} = 1.2755(11)$

$\tau_n(1+3g_A^2) = 5172.0(1.1)$ s

$$\tau_n^{\rm trap} = 879.4(6)\ {\rm s} \to g_A = 1.2756(5),$$
$$\tau_n^{\rm beam} = 888.0(2.0)\ {\rm s} \to g_A = 1.2681(17),$$
$$g_A^{\rm post2002} = 1.2755(11) \to \tau_n = 879.5(1.3)\ {\rm s},$$
$$g_A^{\rm pre2002} = 1.2637(21) \to \tau_n = 893.1(2.4)\ {\rm s}.$$

$\tau_n^{\rm favored} = 879.4(6)$ s $\qquad$ $g_A^{\rm favored} = 1.2755(11)$

- Hayen, PRD **103**, 113001 (2021): update of the so-called "inner *RC*" $[\Delta_R^{V,A}]$ to τ_n

$$|V_{ud}|^2\tau_n(f_V + 3f_A\lambda^2) = \frac{2\pi^3}{G_F^2 m_e^5 g_V^2}\frac{1}{1+RC}$$
$$\lambda = g_A/g_V$$
$$1+RC = 1+\delta_{\rm out}(E)+\Delta_R^V$$
$$g_A = g_A^{\rm QCD}\left[1+\frac{1}{2}(\Delta_R^A-\Delta_R^V)+\delta_{\rm BSM}\right]$$

$\Rightarrow g_A \equiv g_A^{\rm exp} \leftrightarrow g_A^{\rm QCD}$
$\Rightarrow$ not relevant for *pp* fusion

- Use LQCD to compute $g_A \to$ work in progress (Cirigliano *et al.*, arXiv:2202.10439)

After SFII: χEFT calculations (I)

A 1st attempt: Marcucci, Schiavilla, Viviani, PRL **110**, 192503 (2013)

- N3LO potential with $\Lambda = 500, 600$ MeV $\rightarrow$ theoretical uncertainty estimate
- Consistent axial current

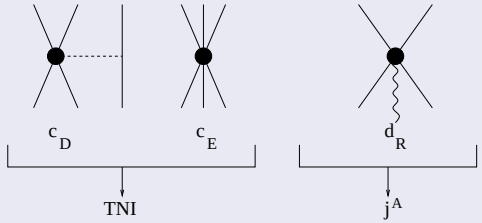

Gardestig & Phillips, PRL **96**, 232301 (2006)

$$d_R = \frac{M_N}{\Lambda_\chi\, g_A} c_D + \frac{1}{3} M_N (c_3 + 2\, c_4) + \frac{1}{6}$$

Gazit, Quaglioni, Navràtil, PRL **103**, 102502 (2009)

- S- and P-waves in the pp state

TABLE I. Cumulative S- and P-wave contributions to the astrophysical S factor at zero c.m. energy in units of 10^{-23} MeV fm^2. The theoretical uncertainties are given in parentheses and are due to the fitting procedure adopted for the LECs in the weak current. The results have been obtained with the two different cutoff values $\Lambda = 500$ and 600 MeV.

	$^1S_0$	$^3P_0$	$^3P_1$	$^3P_2$
$\Lambda = 500$ MeV	4.008(5)	4.011(5)	4.020(5)	4.030(5)
$\Lambda = 600$ MeV	4.008(5)	4.010(5)	4.019(5)	4.029(5)

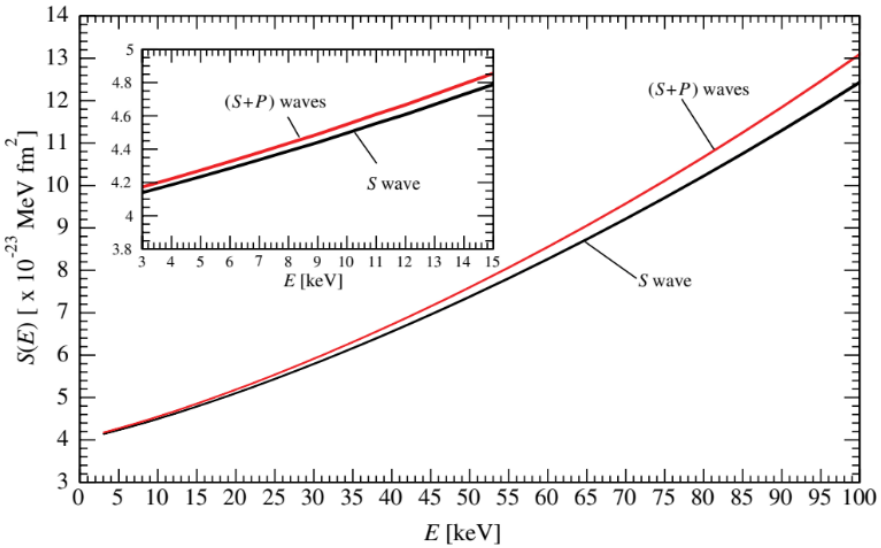

FIG. 2 (color online). The astrophysical S factor as a function of the c.m. energy in the range 0–100 keV. The S- and $(S + P)$-wave contributions are displayed separately. In the inset, $S(E)$ is

After SFII: χEFT calculations (I)

A 1st attempt: Marcucci, Schiavilla, Viviani, PRL **110**, 192503 (2013)

- N3LO potential with $\Lambda = 500, 600$ MeV $\rightarrow$ theoretical uncertainty estimate
- Consistent axial current $\leftarrow$ 1st mistake

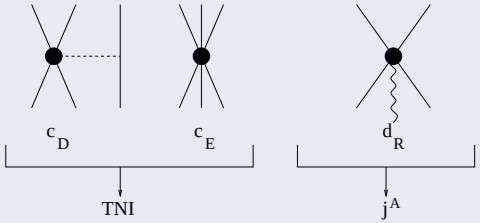

Gardestig & Phillips, PRL **96**, 232301 (2006)

$$d_R = \frac{M_N}{\Lambda_\chi\, g_A} c_D + \frac{1}{3} M_N (c_3 + 2\, c_4) + \frac{1}{6}$$

Gazit, Quaglioni, Navràtil, PRL **103**, 102502 (2009)

- S- and P-waves in the pp state $\leftarrow$ 2nd mistake

TABLE I. Cumulative S- and P-wave contributions to the astrophysical S factor at zero c.m. energy in units of 10^{-23} MeV fm^2. The theoretical uncertainties are given in parentheses and are due to the fitting procedure adopted for the LECs in the weak current. The results have been obtained with the two different cutoff values $\Lambda = 500$ and 600 MeV.

	$^1S_0$	$^3P_0$	$^3P_1$	$^3P_2$
$\Lambda = 500$ MeV	4.008(5)	4.011(5)	4.020(5)	4.030(5)
$\Lambda = 600$ MeV	4.008(5)	4.010(5)	4.019(5)	4.029(5)

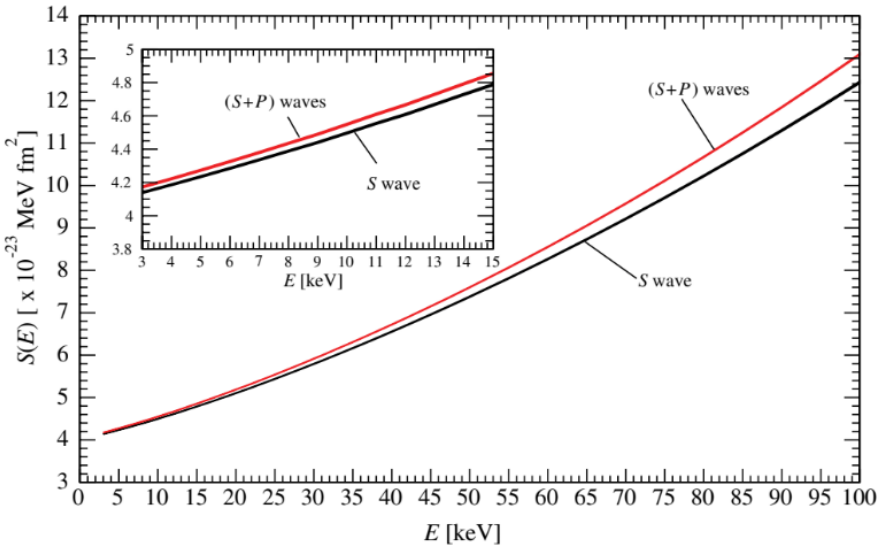

FIG. 2 (color online). The astrophysical S factor as a function of the c.m. energy in the range 0–100 keV. The S- and $(S + P)$-wave contributions are displayed separately. In the inset, $S(E)$ is

1st mistake, found thanks to R. Schiavilla, private communications

$$d_R = \frac{M_N}{\Lambda_\chi\, g_A} c_D + \frac{1}{3} M_N (c_3 + 2\, c_4) + \frac{1}{6} \quad \longrightarrow \quad d_R = -\frac{1}{4} \frac{M_N}{\Lambda_\chi\, g_A} c_D + \frac{1}{3} M_N (c_3 + 2\, c_4) + \frac{1}{6}$$

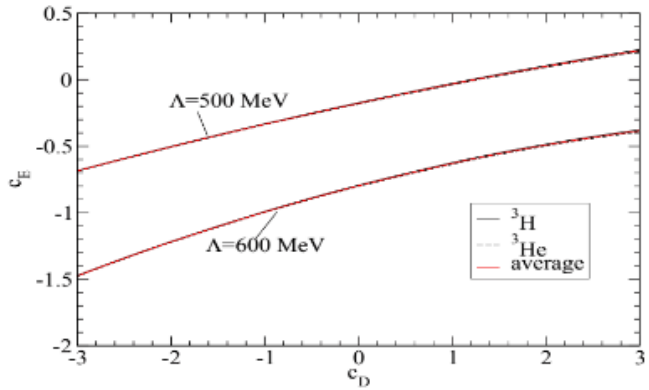

FIG. 1: (Color online) c_D-c_E trajectories fitted to reproduce the experimental ^{3}H and ^{3}He BE's. See text for explanation.

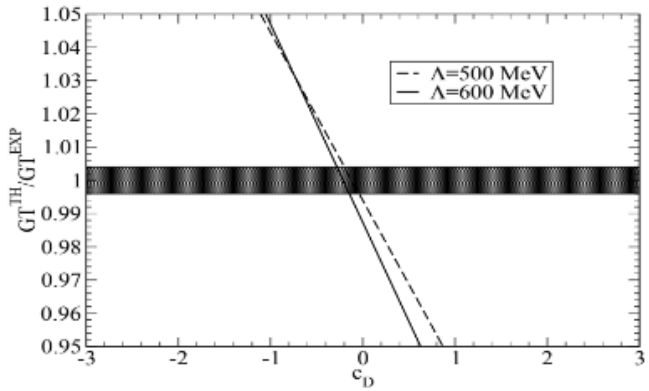

FIG. 2: The ratio GT^{TH}/GT^{EXP} as function of the LEC c_D.

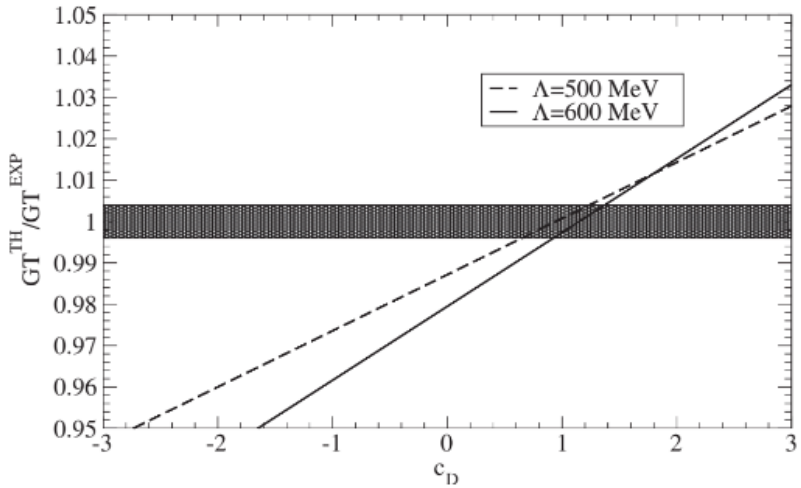

FIG. 1. The ratio GT^{TH}/GT^{EXP} as a function of the LEC c_D.

No effect on **muon capture on *d***

⇓

We expect no effect on *pp* (but ... TBC)

Marcucci *et al.*, PRL **108**, 052502 (2012)

Marcucci *et al.*, PRL **121**, 049901(E) (2018)

2nd mistake, found thanks to Acharya, Platter, Rupak, arXiv:1903.02590

Upon re-examination of the computer programs used for the calculation, we have identified an error in the determination of the P-wave reduced matrix elements (RMEs) associated with the longitudinal multipole operator. These RMEs are denoted as $L_\Lambda^{LSJ}(q)$ in the Letter.

$$L_\Lambda^{LSJ}(q) \to j_z^V(q) \propto \frac{E_f - E_i}{\boldsymbol{q}} \rho^V(q)$$

$\boldsymbol{q}$ in fm^{-1} while $E_f - E_i$ in MeV $\Rightarrow \hbar c$ missing $\Rightarrow L_\Lambda^{LSJ}(q)$ overestimated!!!

TABLE I. Individual S- and P-wave contributions to the astrophysical S factor at zero c.m. energy in units of MeV fm^2. The theoretical uncertainties, given in parentheses, are due to the fitting procedure adopted for the LECs in the weak current and affect essentially only the S-wave contributions. The results have been obtained with the two different cutoff values $\Lambda = 500$ and 600 MeV.

	$^1S_0$	$^3P_0$	$^3P_1$	$^3P_2$
$\Lambda = 500$ MeV	$4.008(5) \times 10^{-23}$	5.5×10^{-30}	1.2×10^{-28}	3.9×10^{-29}
$\Lambda = 600$ MeV	$4.008(5) \times 10^{-23}$	5.4×10^{-30}	1.1×10^{-28}	3.9×10^{-29}

P-wave contributions negligible

Marcucci, Schiavilla, Viviani, PRL **123**, 019901(E) (2019)

$$S_{11}(0) = 4.008(5) \times 10^{-25}\,\mathrm{MeV\ b}$$

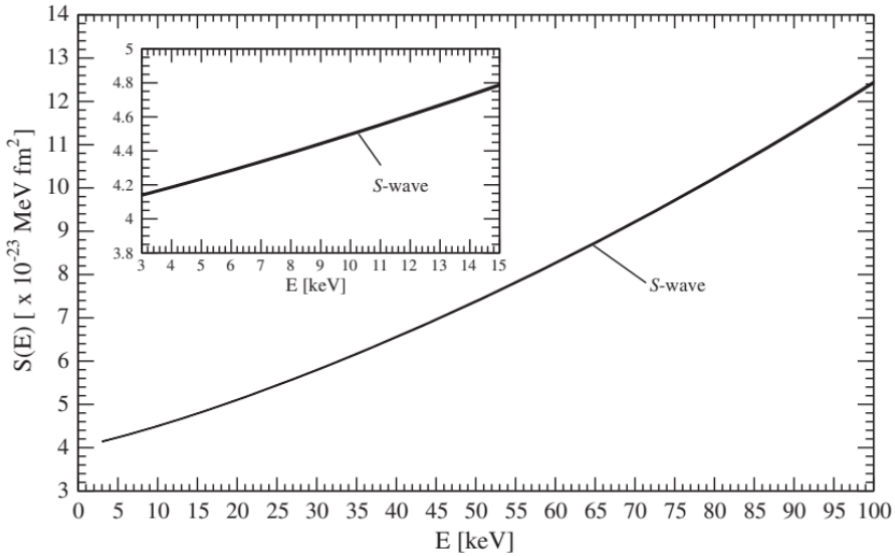

TABLE II. Values for $S^n(0)/S(0)$ with $n = 1$–4, in units of MeV^{-n}, and the χ^2 as defined in the text, obtained with a polynomial fit of $S(E)$ up to orders $O(E^2)$ (Fit 1), $O(E^3)$ (Fit 2), and $O(E^4)$ (Fit 3), retaining only S waves, since the P-wave contributions are negligible. Also listed are the results of Ref. [1]. The theoretical uncertainties, listed only for $n = 1, 2, 3$, are given in parentheses and account for the cutoff sensitivity and the errors due to the LEC's fitting procedure.

n	1	2	3	4	χ^2
Fit 1	12.23(1)	178.4(3)			1.2×10^{-3}
Fit 2	11.42(1)	239.6(5)	−1464(5)		1.9×10^{-4}
Fit 3	10.82(1)	317.4(6)	−5839(9)	98×10^3	2.1×10^{-5}
Ref. [1]	11.3(1)	170(2)			4.7×10^{-1}

However, as we noted in Ref. [6], we expect this error to have a negligible impact on the present predictions. In order to test this expectation, as well as to take into account the most recent developments in both nuclear chiral interactions [7–9] and currents [10], we are in the process of re-examining the pp weak capture *in toto*.

Unfortunately ... yet to be done

Marcucci, Schiavilla, Viviani, PRL **123**, 019901(E) (2019)

After SFII: χEFT calculations (II)

Acharya *et al.*, PLB **760**, 584 (2016)

- consistent χEFT up to N2LO
- error quantification due to
  1. computational method
  2. statistical uncertainties in the LECs
  3. systematic uncertainty due to the variation of the χEFT cutoff
  4. systematic variations in the database used to calibrate V_{NN}
- test of the polynomial extrapolation procedure $\rightarrow S'_{11}(0), S''_{11}(0)$
- statistical correlations between $S_{11}(0)$ and few-nucleon observables

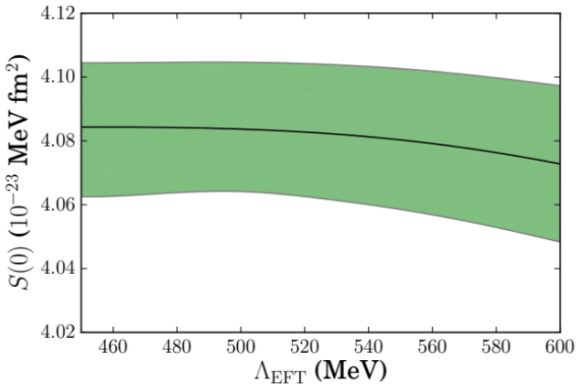

FIG. 2. (Color online). The green band indicates the spread of $S(0)$-values due to variations in $T_{\rm Lab}^{\rm max}$ used in the optimization of the NNLO chiral force, as well as the propagated statistical uncertainties of all LECs and g_A, as a function of the cutoff $\Lambda_{\rm EFT}$ in the χEFT. $\Lambda_{\rm EFT}$ was varied between 450 MeV and 600 MeV in steps of 25 MeV. The cutoff in the current and the interaction sectors were always equal to each other. This figure demonstrates that the S-factor is relatively insensitive to reasonable variations in the cutoff.

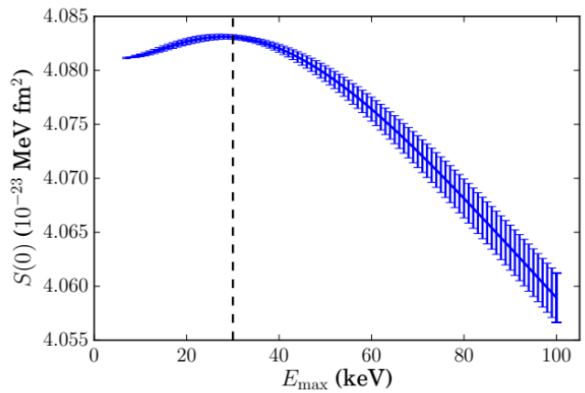

FIG. 1. Extrapolated $S(0)$-values using the cubic polynomial fit. The vertical error bars indicate the statistical uncertainty due to uncertainties in the polynomial fit coefficients. Clearly, they increase rapidly for $E_{\rm max} \gtrsim 30$ keV.

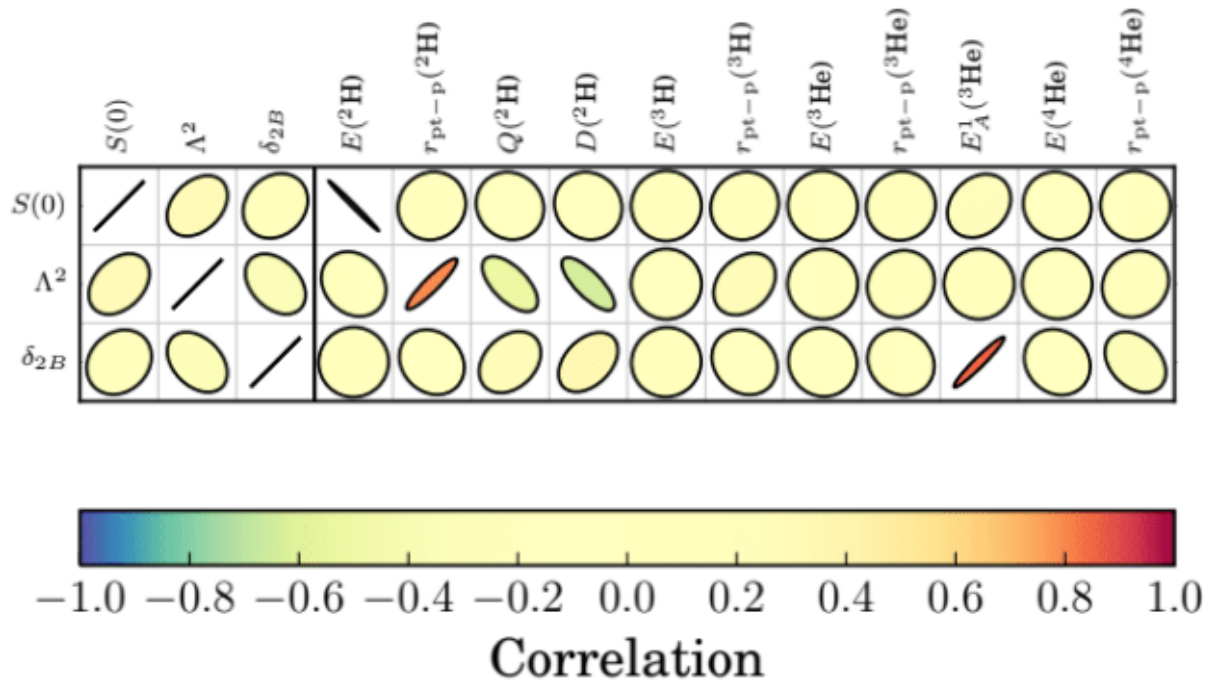

FIG. 3. (Color online). Correlation matrix of the zero-energy S-factor ($S(0)$), the squared radial wave function overlap (Λ^2), and the ratio of the 2B and 1B current matrix elements ($\delta_{2\mathrm{B}}$). We also show the correlations between these quantities and the ground state energies (E), point-proton radii ($r_{\mathrm{pt-p}}$) for $A = 2, 3, 4$ nuclei as well as the matrix element of the reduced axial-vector current (E_A^1) of the triton β-decay and the quadrupole moment ($Q(^2\mathrm{H})$) and D-state probability ($D(^2\mathrm{H})$) of the deuteron.

$$S_{11}(0) = (4.081^{+0.024}_{-0.032}) \times 10^{-25}\ \text{MeV b} \qquad \text{at } \mathcal{O}(\alpha)$$

$$\Downarrow$$

$$S_{11,\text{cor}}(0) = (4.047^{+0.024}_{-0.032}) \times 10^{-25}\ \text{MeV b} \qquad \text{at } \mathcal{O}(\alpha^2)\ [\text{estimated}^*]$$

* Schiavilla *et al.*, PRC **58**, 1263 (1998)

$$S'_{11}(0)/S_{11}(0) \rightarrow 10.84(2)\ \text{MeV}^{-1}$$
$$S''_{11}(0)/S_{11}(0) \rightarrow 317.8(13)\ \text{MeV}^{-2}$$

Some remarks:

- Fitting range $E = 0 - 30$ keV
- d_R still "old" (-1/4 missing) ...

$$\hat{d}_R = \frac{1}{m_N}\frac{c_D}{g_A \Lambda_{\text{EFT}}} + \frac{1}{3m_N}(c_3 + 2c_4) + \frac{1}{6}$$

After SFII: χEFT calculations (III)

Effect of truncated Hilbert space: Acharya *et al.*, PRC **95**, 031301(R) (2017)

- study of the long-distance asymptotic of Ψ_d
- IR truncation effect $\rightarrow L$

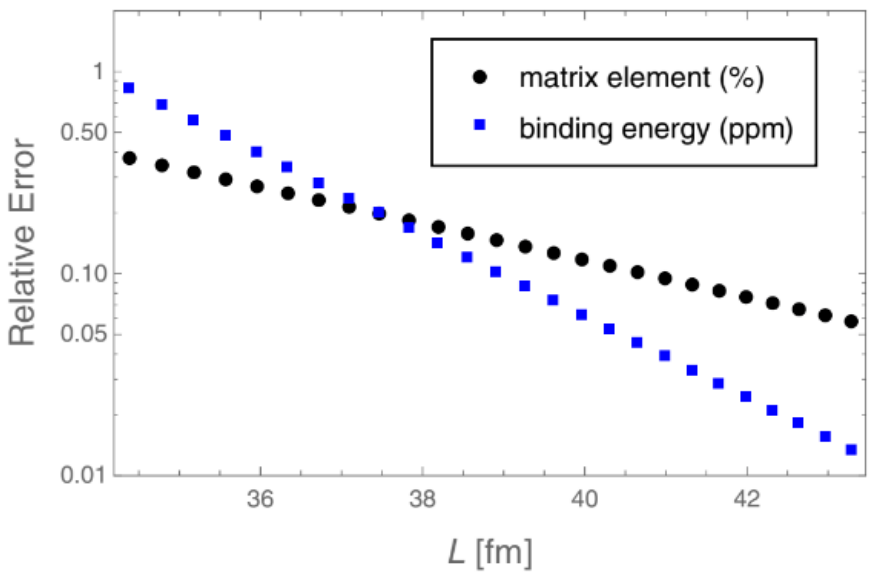

FIG. 1. IR truncation error in the axial-vector matrix element of *pp* fusion at 50-keV center-of-mass energy (black circles) and in the deuteron binding energy (blue squares). The relative errors for the axial-vector matrix elements and those for the binding energy are expressed in percentage and parts per million (ppm) respectively.

In Fig. 1, we plot the relative error due to a IR cutoff in the matrix element of the Gamow-Teller operator between the deuteron s-wave and the pp $^1S_0$ wave functions at 50-keV center-of-mass energy, $\Delta\mathcal{I}_0(k;\eta;L)/\mathcal{I}_0(k;\eta;\infty)$. For comparison, we also show the relative IR truncation error in the deuteron binding energy. The error in the matrix element at $L = 35$ fm is about 0.3%, which translates to an error in the cross section of about 0.6%. The size of this error is relevant for computing pp fusion cross sections to percentage precision, which recent calculations [6] aim at. In contrast, the deuteron

After SFII: $\not\pi$EFT calculations (I)

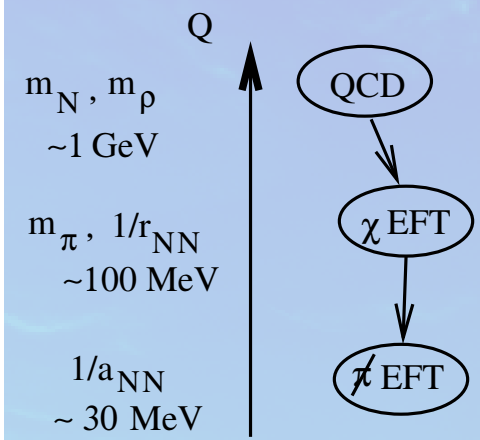

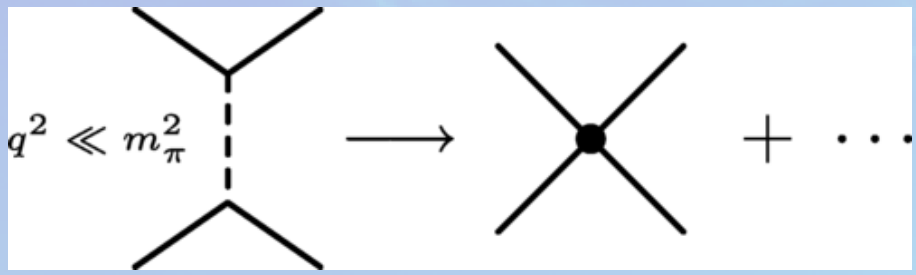

Hammer, König, van Kolck, RMP **92**, 025004 (2020)

Chen, Liu, Hu, PLB **720**, 385 (2013) → N2LO

- re-calculation of $S_{11}(0)$ using
  - updated $g_A = 1.2695$
  - solar $\nu_e d$ & reactor $\overline{\nu}_e d$ breakup data → $L_{1,A} = (3.4 \pm 3.7)$ fm^3
- first calculation of $S'_{11}(0)/S_{11}(0)$ & $S''_{11}(0)/S_{11}(0)$ → **insensitive to $L_{1,A}$**

$$\mathrm{S}_{11}(0) = (3.99 \pm 0.14) \times 10^{-25}\,\mathrm{MeV\,b}\,,$$

$$\mathrm{S}'_{11}(0) = \mathrm{S}_{11}(0)\,(11.3 \pm 0.1)\ \mathrm{MeV}^{-1}\,,$$

$$\mathrm{S}''_{11}(0) = \mathrm{S}_{11}(0)\,(170 \pm 2)\ \mathrm{MeV}^{-2}\,.$$

The importance of muon capture on deuteron

$$\mu^- + d \to n + n + \nu_\mu$$

$$\frac{d\Gamma}{dE} = f(L_{1,V}; L_{1,A})$$

- $L_{1,V} = -4.08$ fm $[n + p \to d + \gamma]$
- $L_{1,A} = 4.0 \pm 6.3$ fm^3 [SNO & SK data*]

* Chen, Heeger, Robertson, PRC **67**, 025801 (2003)

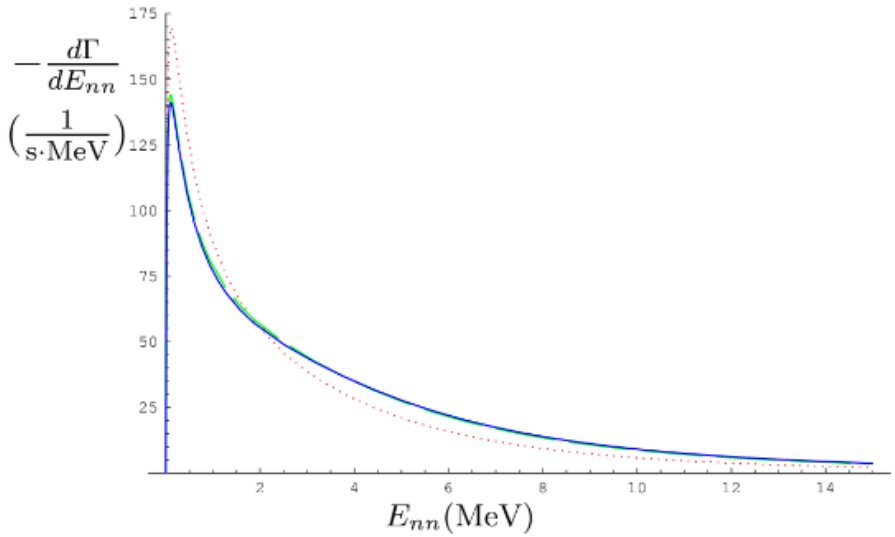

FIG. 2: (Color online) The differential capture rate $d\Gamma/dE_{nn}$ calculated using $L_{1,A} = 6$ fm^3. The doted line is the LO result. The dashed and solid lines, which sit on top of each other in this scale, are the NLO and N^{2}LO results, respectively.

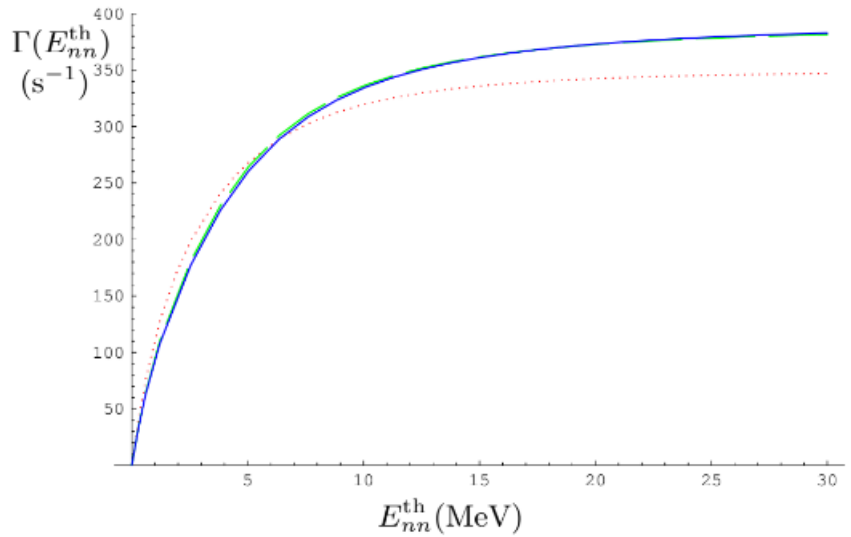

FIG. 3: (Color online) The integrated capture rate $\Gamma(E_{nn}^{\text{th}})$ calculated using $L_{1,A} = 6$ fm^3 for the relative energy E_{nn}^{th} of the two neutrons up to 30 MeV. The description of the lines is the same as that in the caption of Fig. 2.

$$\Gamma(E_{nn}^{\text{th}}) \equiv -\int_0^{E_{nn}^{\text{th}}} \frac{d\Gamma}{dE_{nn}} dE_{nn} \Rightarrow \Gamma(E_{nn}^{\text{th}}) = a(E_{nn}^{\text{th}}) + b(E_{nn}^{\text{th}}) L_{1,A}$$

Table 1:
Coefficients functions $a(E_{nn}^{\rm th})$ and $b(E_{nn}^{\rm th})$ for specific values of two-neutron relative energy $E_{nn}^{\rm th}$ from the EFT($\not\pi$) calculation.

$E_{nn}^{\rm th}$(MeV)	5.0	10.0	15.0	20.0
$a(E_{nn}^{\rm th})(\mathrm{s}^{-1})$	239.2	308.0	332.0	342.3
$b(E_{nn}^{\rm th})(\mathrm{s}^{-1}\mathrm{fm}^{-3})$	3.3	4.2	4.7	4.9

$\Gamma(E_{nn}^{\rm th})$ within 2 % experimental error $\rightarrow$ $L_{1,A}$ within $\pm$2.0 fm^3

Chen, Inoue, Ji, Li, PRC **72**, 061001 (2005)

Theoretical framework $pp \longleftrightarrow \mu^- + d$

χEFT-1: Marcucci *et al.*, PRL **110**, 192503 (2013) / PRL **123**, 019901(E) (2019)
$\longleftrightarrow$ PRL **108**, 052502 (2012) / PRL **121**, 049901(E) (2018)

χEFT-2: Acharya *et al.*, PLB **760**, 584 (2016)
$\longleftrightarrow$ PRC **98**, 065506 (2018)

$\not\pi$EFT: Chen *et al.*, PLB **520**, 87 (2001) + PLB **720**, 385 (2013)
$\longleftrightarrow$ PRC **72**, 061001 (2005)

After SFII: $\not\pi$EFT calculations (II)

Behzadmoghaddam, Bayegan, Arani, EPJA **56**, 158 (2020): $\not\pi$EFT with new PC up to NLO

- Old PC
  - (Q/M_{hi}), with $M_{hi} \sim 1$ GeV
  - ${}^1S_0 \rightarrow$ shallow virtual bound state
- New PC
  - $\delta({}^1S_0) \rightarrow 0$ for $k \sim 340$ MeV $(k < M_{hi})$

  $\Rightarrow$ different kind of fine-tuning

  $\rightarrow$ new PC rearrangement in order to
    - get the existence of the zero amplitude at LO
    - get the shallow virtual state

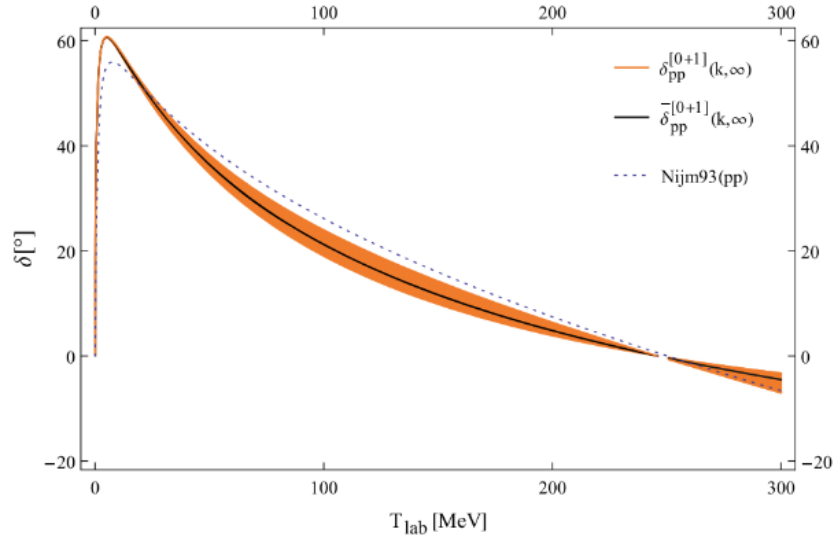

Fig. 5 pp ${}^1S_0$ phase shift (in degrees), against laboratory energy at NLO. The black solid line illustrates the analytical result, Eq. (38) with $\Lambda \rightarrow \infty$, and the value of the shape parameter from Ref. [65]. While the orange band around it shows a $\pm 30\%$ variation in this value. The black dotted line are the Nijm93 results [54,60]

$$l_{1,A} = 0.86 \pm 0.05 \rightarrow \text{from } M^{1b}/M^{2b*}$$

* Park *et al.*, PRC **67**, 055206 (2003)

$$S_{11}^{[\mathrm{LO}]}(0) = 3.51 \times 10^{-25} \text{ MeV b}$$
$$S_{11}^{[\mathrm{NLO}]}(0) = 3.57 \times 10^{-25} \text{ MeV b}$$

After SFII: $\not$EFT calculations (III) $\rightarrow$ P-waves

Acharya, Platter, Rupak, PRC 100, 021001 (2019)

- Study of P-waves up to NLO
- $S_{11,P}(0) = (2.47 \pm 0.25 \pm 0.01) \times 10^{-30}$ MeV b
- $S'_{11,P}(0) = (2.16 \pm 0.22 \pm 0.01) \times 10^{-28}$ b

$\Rightarrow$ P-waves negligible $\Rightarrow$ $S_{11}(0) = (4.047^{+0.024}_{-0.032}) \times 10^{-25}$ MeV b

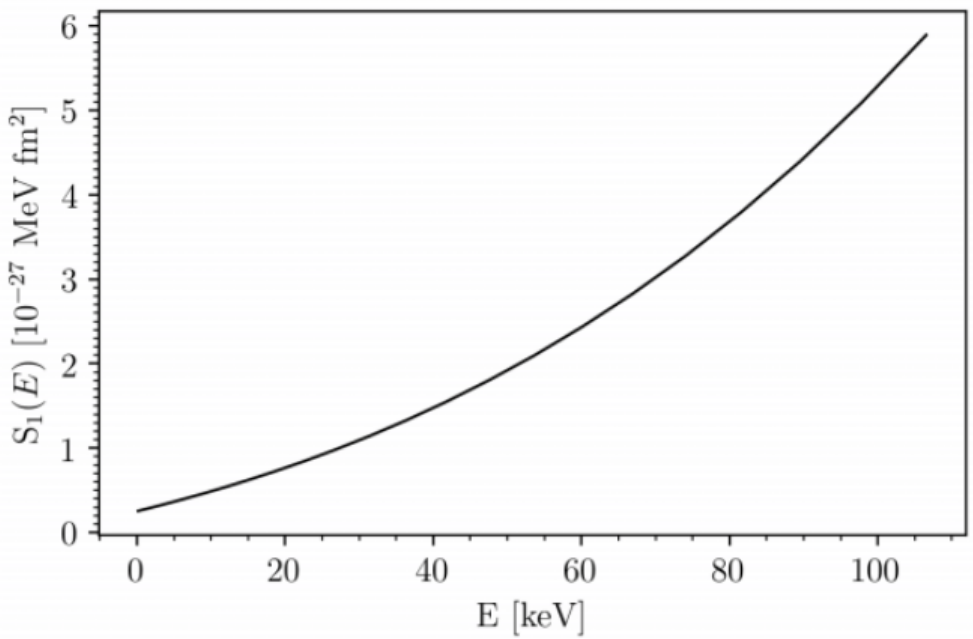

After SFII: $\not$EFT calculations (IV) $\rightarrow l_{1,A}$

De-Leon, Platter, Gazit, PRC **100**, 055502 (2019)

- ^{3}H β-decay up to NLO
- uncertainty estimates from
  - g_A
  - triton β-decay half life $\tau_{1/2}$
- Effective Range Expansion & Z-parametrization

$$A_S = \sqrt{2\gamma_t Z_d}$$
$$\gamma_t = \sqrt{M E_b(d)}$$

	ERE		Z-parametrization
$Z_d^{\rm LO}$	$=$ 1	$Z_d^{\rm LO}$	$=$ 1
$Z_d^{\rm NLO}$	$\simeq$ 1.408	$Z_d^{\rm NLO}$	$=$ 1.690(3)

$$l_{1,A}^{\rm ERE} = 0.312 \pm 0.004 \pm 0.004 \pm 0.001$$
$$l_{1,A}^{\rm Z} = 0.051 \pm 0.004 \pm 0.004 \pm 0.001 \ ,$$

Consequences for $S_{11}(0)$ in De-Leon & Gazit, arXiv:2207.10176

After SFII: $\not\pi$EFT calculations (V) $\rightarrow L_{1,A}$

Acharya & Bacca, PRC **101**, 015505 (2020)

- NC and CC $\bar{\nu}/\nu - d$ scattering in χEFT up to 150 MeV
- uncertainty estimates from
  - χEFT truncation of the EW current
  - χEFT cutoff Λ
  - Fitting database
- high-precision $\nu - d$ predictions for $E > 100$ MeV requires precise $g_A(Q)$
- matching χEFT-$\not\pi$EFT for low energy

$$L_{1,A} = 4.9^{+1.9}_{-1.5}\ \text{fm}^3$$

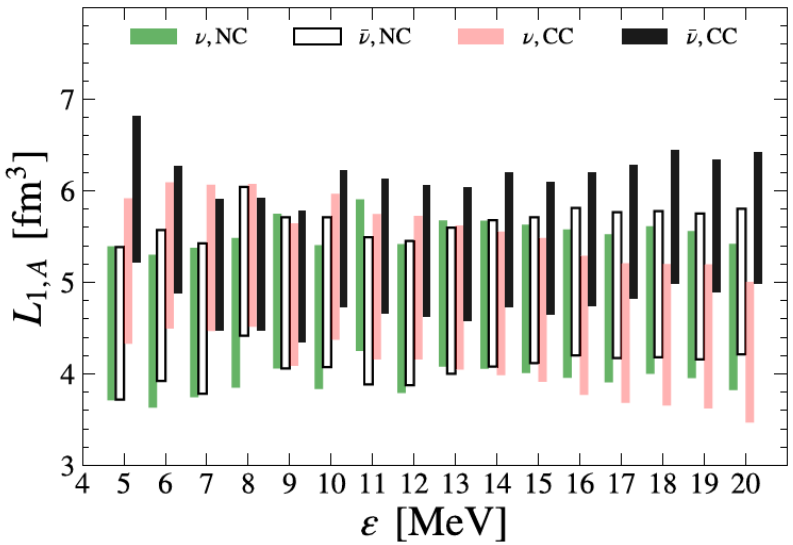

FIG. 3. The $L_{1,A}$ values determined from ν NC (green/dark grey), $\bar{\nu}$ NC (white), ν CC (red/light grey), and $\bar{\nu}$ NC (black) processes. The vertical spreads of the bands are the NNLO_{sim} uncertainties. The $L_{1,A}$ values were calculated at 1 MeV intervals in the 5–20 MeV range of $\bar{\nu}/\nu$ energies, but have been slightly displaced along the horizontal axis for visibility.

After SFII: lattice calculations(I)

LEFT: Rupak & Ravi, PLB **741**, 301 (2015)

- LO strong+Coulomb interaction

$$V_s(\boldsymbol{r}) = c_0\delta(\boldsymbol{r})$$
$$V_C(\boldsymbol{r}) = \frac{\alpha}{r}$$

- V_C regularized for $r \to 0$ $[V_C(r \to 0) \to d_0\delta(\boldsymbol{r})]$
- spherical wall method $\to \delta_0(k)$
- $\Lambda(k) \propto |\int d^3r\psi_d^*(\boldsymbol{r})\psi_{pp}(\boldsymbol{r})|$
- $\Lambda^{(\mathrm{latt})}(0) = 2.49 \pm 0.02$ vs. $\Lambda^{(\mathrm{SFII})}(0) = 2.65 \pm 0.01$

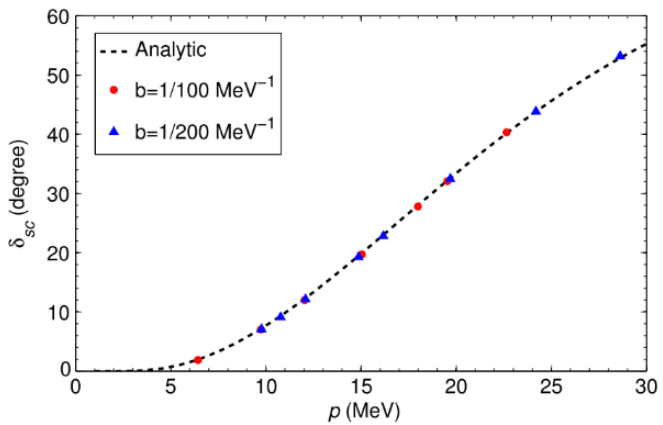

Fig. 1. Coulomb subtracted phase shift. The dashed curve is the analytical result from Eq. (9). The red circle data correspond to $b = 1/100$ MeV^{-1}, $\hat{c}_0 + \hat{d}_0 = -0.4047$, and the blue triangle data correspond to $b = 1/200$ MeV^{-1}, $\hat{c}_0 + \hat{d}_0 = -0.8330$ lattice results, respectively. (For interpretation of the references to color in this figure legend, the reader is referred to the web version of this article.)

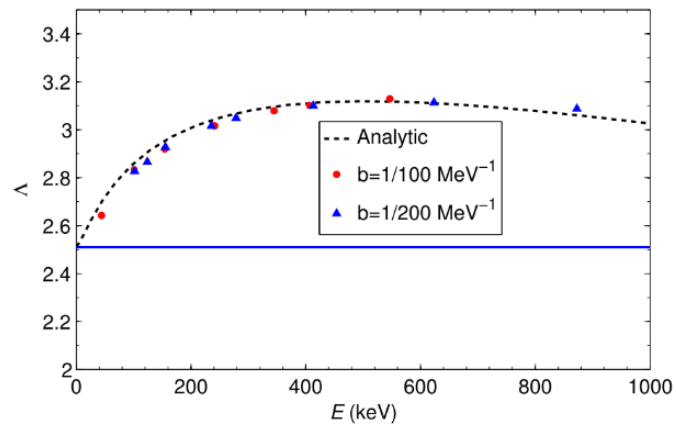

Fig. 2. Proton–proton fusion rate. The dashed curve is the analytical result. Red circles and blue triangles show lattice data at $b = 1/100$ MeV^{-1} and $b = 1/200$ MeV^{-1} with the lattice couplings from Fig. 1. The horizontal grid line at $\Lambda = 2.51$ indicates the LO continuum EFT result at zero energy [27,28]. (For interpretation of the references to color in this figure legend, the reader is referred to the web version of this article.)

After SFII: lattice calculations (II)

LQCD: Savage *et al.* (NPLQCD Collab.), PRL **119**, 062002 (2017)

- addressed ^{3}H β-decay (GT) and *pp*
- SU(3)-flavor symmetric value of the quark masses $\rightarrow m_\pi \sim 806$ MeV
- GT$=0.979(03)(10)$ at these quark masses (within 2σ of GT^{exp})
- $\langle {}^3S_1; J_z = 0 | A_3^3 | {}^1S_0; I_z = 0 \rangle / Z_A = 2.568(5)(31)$

$\Rightarrow$ assuming small quark mass dependence $\Lambda = 2.659(2)(9)(5)$ vs. $\Lambda^{\rm SFII} = 2.65(1)$

$\Rightarrow$ $L_{1,A} = 3.9(0.2)(1.0)(0.4)(0.9)$ fm^3

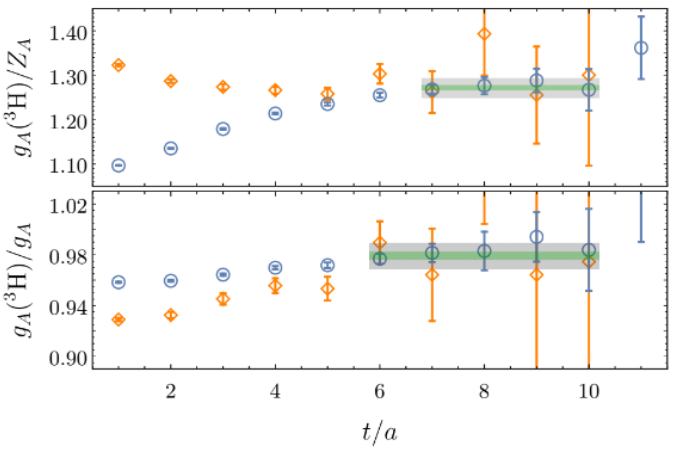

FIG. 2. The ratios of correlation functions that determine the unrenormalized isovector axial matrix element in ^{3}H (upper panel), and the ratio of the isovector axial matrix element in ^{3}H to that in the proton (lower panel). The orange diamonds (blue circles) correspond to the SS (SP) effective correlator ratios and the bands correspond to constant fits to the asymptotic behavior.

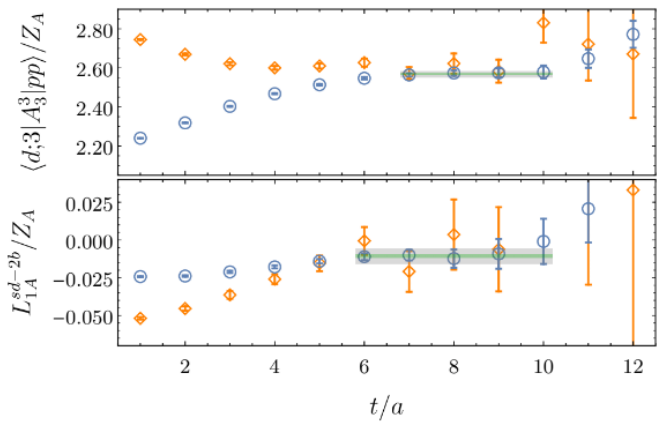

FIG. 3. The ratios of correlation functions that determine the unrenormalized isovector axial matrix element in the $J_z = I_z = 0$ coupled two-nucleon system (upper panel), and the unrenormalized difference between the axial matrix element in this channel and $2g_A$ (lower panel). The orange diamonds (blue circles) correspond to the SS (SP) effective correlator ratios and the bands correspond to fits to the asymptotic plateau behavior and include only the statistical and fitting systematic uncertainties (the additional 1% uncertainty from Wigner symmetry breaking is not represented in the bands).

A recent analysis of *pp* fusion:

Gaspard, Sparenberg, Wenda, Baye, PRC **100**, 035805 (2019)

- $V_{NN} \rightarrow$ AV18, Reid93, NijmII
- $d \rightarrow {}^3S_1$ & only one-body axial current
- **energy-dependence** analysis of $\Lambda(E)$

$$F_{\eta,0}\cos\delta_0 + G_{\eta,0}\sin\delta_0 = \frac{C_{\eta,0}/(2\eta)}{|\Delta_0^+(E)|}\left(\frac{a_B}{2}\varkappa_0\Phi_{\eta,0} + \Psi_{\eta,0}\right)$$

$$\varkappa_0(E) \simeq \frac{-1}{\alpha_0} + \frac{r_0}{2}\frac{m_p}{\hbar^2}E$$

$$\Delta_0^+(E) = \left(\frac{a_B}{2}\varkappa_0 - g_{\eta,0}\right) - \frac{i\pi}{e^{2\pi\eta}-1}$$

$$\frac{\Lambda'(0)}{\Lambda(0)} = 1.106(2) + 0.1981(1)\,(|\alpha_0| - 7.815) \rightarrow 1.106(3)\ \mathrm{MeV}^{-1}$$

$$\frac{\Lambda''(0)}{\Lambda(0)} = 32.795(6) + 4.758(2)\,(|\alpha_0| - 7.815) \rightarrow 32.80(5)\ \mathrm{MeV}^{-2}$$

$$S_{11}(0) = (3.95 \pm 0.03) \times 10^{-25}\ \mathrm{MeV\ b}$$
$$S'_{11}(0) = S_{11}(0)(11.25 \pm 0.01)\ \mathrm{MeV}^{-1}$$
$$S''_{11}(0) = S_{11}(0)(169.5 \pm 0.03)\ \mathrm{MeV}^{-2}$$

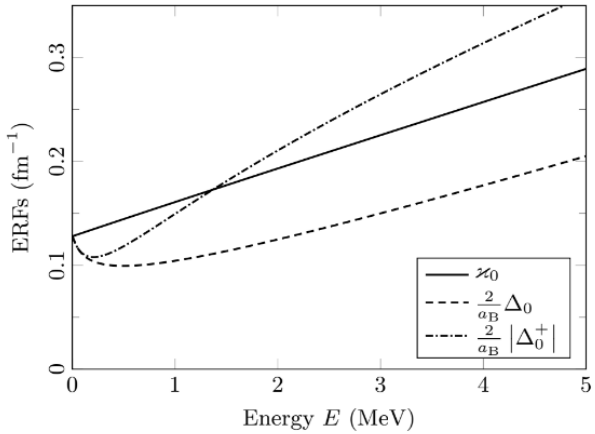

FIG. 2. Effective-range functions of the proton-proton $^1S_0$ scattering for the Reid93 potential [23]. The other potential models provide very close curves at this scale.

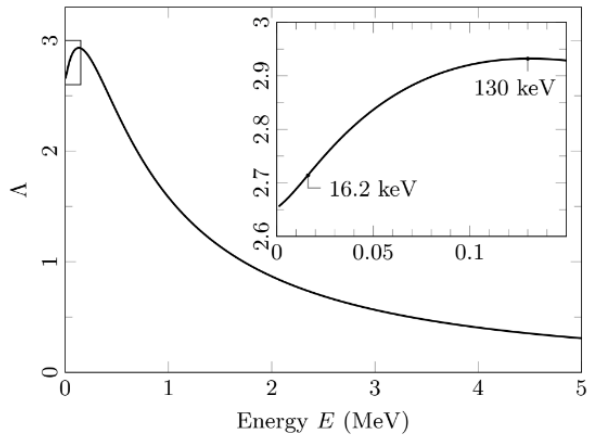

FIG. 5. Matrix element Λ of the weak capture computed with the Reid93 potential. The curve has an inflection point at 16.2 keV and a maximum at 130 keV. The inset is an enlargement of the graph to low energy.

The *hep* reaction: SFII

$$p + {}^3\mathrm{He} \rightarrow {}^4\mathrm{He} + e^+ + \nu_e$$

- $\langle p + {}^3\mathrm{He}|GT|{}^4\mathrm{He}\rangle$ suppressed due to *s*-wave orthogonality
- $p + {}^3\mathrm{He}$ scattering $\rightarrow$ CHH method
- phenomenological[1] and EFT*[2] calculations
- $S_{\mathrm{hep}}(0) = (8.6 \pm 2.6) \times 10^{-20}$ keV b

[1] Marcucci *et al.*, PRC **63**, 015801 (2000)

[2] Park *et al.*, PRC **67**, 055206 (2003)

SFII recommendations

- new *hep* study with broad spectrum of Hamiltonian models
- study of related EW reactions (for instance $\mu^- + {}^3\mathrm{He} \rightarrow {}^3\mathrm{H} + \nu_\mu$) ✓
- further work to understand the relation *hep* − *hen* [$n + {}^3\mathrm{He} \rightarrow {}^4\mathrm{He} + \gamma$]

No new calculations since SFII!!

Electron capture by ^{7}Be & *pep*: SFII

$R(^7\mathrm{Be} + e^-)$

- EC $\rightarrow$ $^7\mathrm{Li}(3/2^-)$ & $^7\mathrm{Li}^*(1/2^-, 478\ \mathrm{keV})$
- Solar EC rate normalized to terrestrial EC rate
  - $\Rightarrow$ no nuclear physics dependence
  - $\Rightarrow$ dependence on e^- probab. densities averaged over the nucleus
    - $\Rightarrow$ calculation of the atomic prob. densities for K and L terrestrial EC rates
    - $\Rightarrow$ solar electron continuum [Debye-Hückel (DH) approximation for plasma screening]
    - $\Rightarrow$ corrections from incomplete ionization
- Bahcall & Moeller, ApJ **155**, 511 (1969) + updates (valid for $10 < T_6 < 16$)

$$R(^7\mathrm{Be} + e^-) = 5.60(1 \pm 0.02) \times 10^{-9} \quad (\rho/\mu_e) \quad T_6^{-1/2}[1 + 0.004(T_6 - 16)]\ \mathrm{s}^{-1}$$

ρ=density
T_6= temperature in 10^6 K
μ_e = mean molecular weight per electron

2% uncertainty $\rightarrow$

- possible corrections to the DH approximation
- possible corrections to terrestrial screening (L/K ratio)

$R(pep)$

- $R(pep)$ normalized to $R(pp)$ [Bahcall & May ApJ **155**, 501 (1969)]

+ radiative corrections [Kurylov *et al.*, PRC **67**, 035502 (2003)] (valid for $10 < T_6 < 16$)

$$R(pep) = 1.130(1 \pm 0.01) \times 10^{-4} \ (\rho/\mu_e) \ T_6^{-1/2}[1 + 0.02(T_6 - 16)]R(pp)$$

EC for CNO isotopes (^{13}N, ^{15}O, ^{17}F)

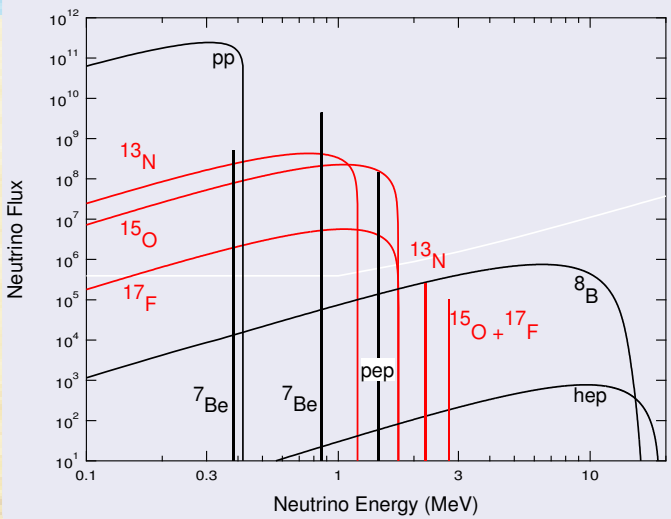

- Bahcall, PRD **41**, 2964 (1990): only capture from continuum
- Stonehill *et al.*, PRC **69**, 015801 (2004): also capture from bound states
- still EC components $\sim 10^{-3}$ β^+ components
- but in a region with only ^{8}B neutrinos

After SFII

Simonucci, Taioli, Palmerini, Busso, ApJ **764**, 118 (2013): e^--density at the nucleus

- "traditional" model: classical non-interacting e^--gas, screened using the DH model ($\lambda_D > \lambda_{\rm DB}$)
- in the Sun $\lambda_D \sim \lambda_{\rm DB}$
- new computation $\rightarrow$ mean-field "adiabatic" approximation to the scattering process
  1. decay rate $\propto \rho_e(0) \rightarrow$ system of coupled HF eqs. for p & e^- in the ^{7}Be electrostatic field
  2. coupling from the self-consistent Hartree term
  3. μ_p & μ_e chosen so that system is neutral far from ^{7}Be atom
  4. $p - {}^7\mathrm{Be}$ and $e^- - {}^7\mathrm{Be}$ scattering=two-body problem + rest=mean field

Table 1
Values (in Atomic Units) of the Electron Density at the Be Nucleus $\rho_e(0)$ for Different Levels of the Theory (HF: Hartree–Fock; TF: Thomas–Fermi; PB: Poisson–Boltzmann; DH: Debye–Hückel) for Solar Conditions ($T = 16$ MK)

$\rho_{\rm HF}(0)$	$\rho_{\rm TF}(0)$	$\rho_{\rm PB}(0)$	$\rho_{\rm DH}(0)$
16.320 ± 0.020	16.135 ± 0.025	14.870 ± 0.020	16.085 ± 0.025

Notes. The conditions at which we performed the calculations are $T = 15.67$ MK, $\rho = 152.9$ g cm^{-3}, $X_{\rm H} = 0.34608$, and $X_{\rm He} = 0.63368$.

Vescovi *et al.*, AA **623**, A126 (2019): effects on solar neutrino fluxes

$$R(^7\mathrm{Be} + e^-) = \frac{\rho}{\mu_e}\kappa \;\; T_6^{-1/2}\left[1 + \alpha(T_6 - 16) + \beta\,\frac{\rho}{\mu_e}[1 + \gamma(T_6 - 16)]\right] \;\; \mathrm{s}^{-1}$$

Table 2. Coefficients for the analytical approximation to the STPB13 and ADE11 electron-capture rates.

	κ	α	β	γ
this paper	5.9065×10^{-9}	-1.3614×10^{-2}	-9.2042×10^{-4}	-1.5334×10^{-1}
ADE11	5.6×10^{-9}	$+4 \times 10^{-3}$	0	0

Table 4. This table presents the predicted fluxes, in units of 10^{10} (pp), 10^9 (^{7}Be), 10^8 (pep, ^{13}N, ^{15}O), 10^6 (^{8}B, ^{17}F), and 10^3 (hep) cm^{-2}s^{-1} for the reference ADE11 models, presented in Table 3, for the STPB13 models and relative differences. .

	GS98			PLJ14		
	ADE11	STPB13	relative differences	ADE11	STPB13	relative differences
Φ(pp)	5.99	5.99	+0.20‰	6.01	6.01	+0.01‰
Φ(pep)	1.42	1.42	+0.25‰	1.43	1.43	+0.01‰
Φ(hep)	8.09	8.09	+0.15‰	8.22	8.22	+0.01‰
$\Phi(^7\mathrm{Be})$	4.74	4.74	+0.38‰	4.54	4.54	-0.01‰
$\Phi(^8\mathrm{B})$	5.28	5.42	+2.70%	4.82	4.95	+2.60%
$\Phi(^{13}\mathrm{N})$	2.82	2.82	+0.67‰	2.55	2.55	+0.06‰
$\Phi(^{15}\mathrm{O})$	2.07	2.07	+0.71‰	1.82	1.82	+0.07‰
$\Phi(^{17}\mathrm{F})$	5.35	5.35	+0.80‰	3.95	3.95	+0.07‰

LOONEY TUNES
"That's all Folks!"
CLAMPETT

Thanks to Jiunn-Wei
and the WG1 participants

Thanks to Jiunn-Wei
and the WG1 participants

Thank you for your attention!